## SUPPLEMENTAL INFORMATION

### Supplemental Figures

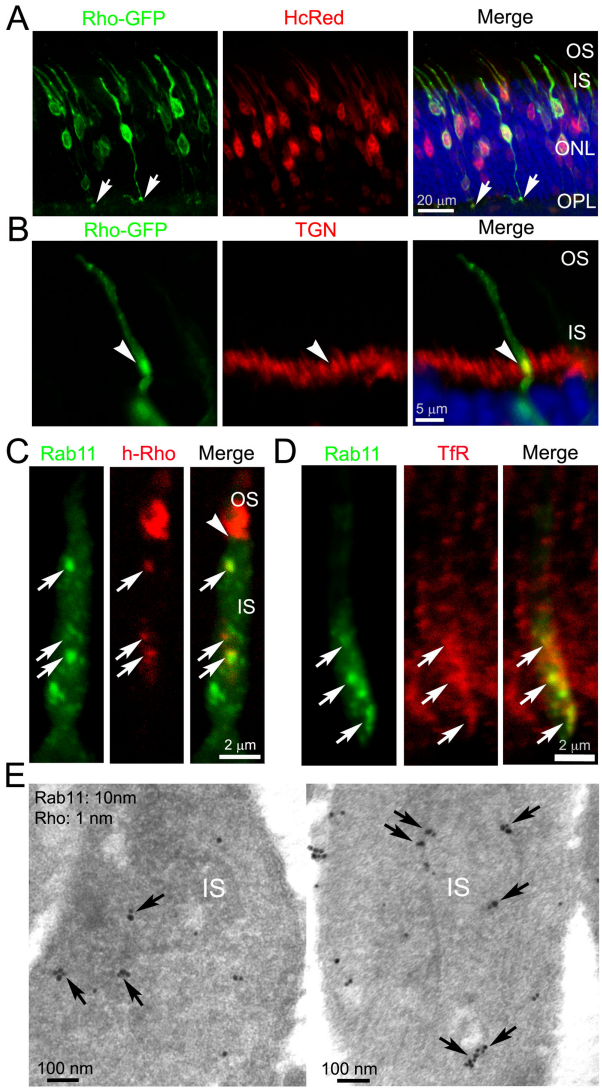


**Fig. S1 Newly synthesized rhodopsin transits through Rab11a-positive intermediate compartments.** Related to Figure 1. (**A**) A retinal slice containing rods transfected with $P_{CAG}$-HcRed and $iP_{CAG}$-Rho-GFP and harvested 12 hr after 4OH induction (8-hr light followed by 4-hr dark). ONL: outer nuclear layer; OPL: outer plexiform layer. Arrows point to the Rho-GFP at the synapses of transfected rods. (**B**) Immunolabeling by TGN38 (red) of a retinal slice containing a rod expressing Rho-GFP for 12 hr. Newly synthesized rhodopsin was widely distributed, in addition to its TGN location (arrowheads) in the IS. (**C**) Immunolabeling of hRho (red) of a rod co-expressing Rab11a-GFP and hRho for 12 hr. Arrows point to the close association between h-Rho and Rab11 signals; an arrowhead marks the IS-OS junction. (**D**) Immunolabeling of transferrin receptor (TfR) in a rod expressing Rab11a-GFP. Arrows point to the overlapping labeling of TfR and Rab11. (E) Two representative electron micrographs revealing the IS regions of CD1 mouse rods labeled for rhodopsin (using 1D4 mAb and detected by 1 nm-gold conjugated anti-mouse Ab) and Rab11a (using anti-Rab11a rabbit Ab and detected by 10 nm-gold conjugated anti-rabbit Ab). Silver enhancement (45 sec) was used for the immunogold detection. Black arrows point to the colocalization of small and large gold particles.

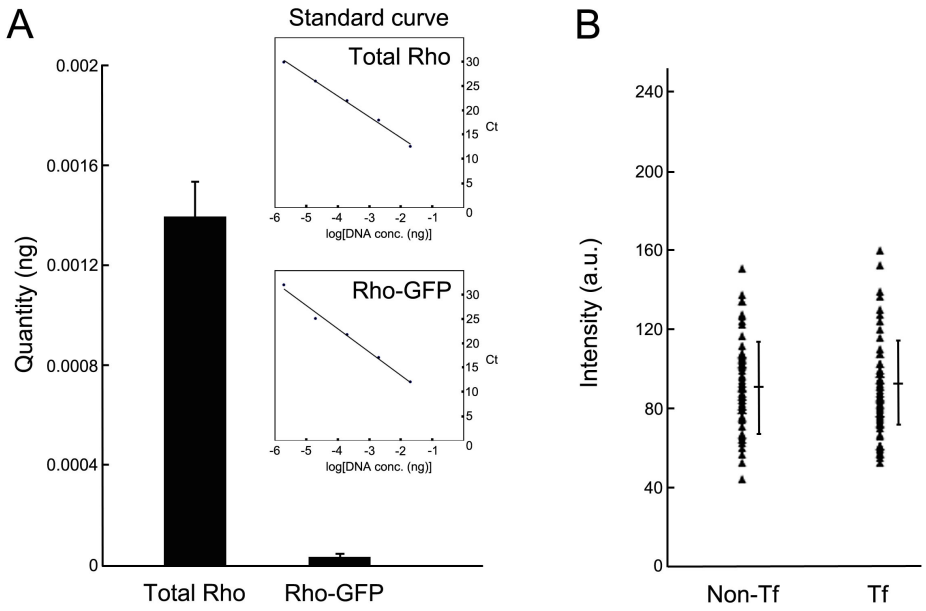


**Fig. S2 Quantification of the expression level of transfected rhodopsin.** Related to Figure 2. (**A**) Three rat retinas transfected with $P_{CAG}$-Rho-GFP were dissociated with collagenase I (1 mg/mL, Worthington) in DMEM/5%FBS at 37°C and triturated gently with fire-polished Pasteur pipets. The supernatant was centrifuged over 10 mL of cold PBS/1%FBS at 1,200 rpm for 10 min at 4°C. The cell pellet was resuspended in cold PBS/1%FBS for FACS. About 30,000 GFP-positive cells were collected; these cells were observed under light microscopy to confirm that ~100% of them were GFP-positive. RNA was isolated from these rods (Qiagen RNeasy Plus Mini kit). Primary cDNAs were obtained using Random hexamer-primed Superscript reverse transcriptase kit (Invitrogen). qRT-PCR was performed using Power SYBR-Green (Applied Biosystems) method. Primers used to detect total rhodopsin and Rho-GFP are 5'-TACATGTTCGTGGTCCACTT (forward)/5'-TTGGAGCCCTGGTGGGTAAA (reverse) and 5'-ACCGTGTCCAAGACGGAGA (forward)/5'-GAAGTCGTGCTGCTTCATGTG (reverse), respectively. The quantities of Rho-GFP and total rhodopsin were obtained by extrapolating Ct values of data points from a standard curve generated using serially diluted $P_{CAG}$-Rho-GFP plasmid of known concentrations. For example, cDNA derived from 1 μL of reverse-transcriptase reaction contains $1.4 \times 10^{-3}$ ng of total rhodopsin and $2.7 \times 10^{-5}$ ng of Rho-GFP. The histogram shows the relative expression level of Rho-GFP and total rhodopsin derived from the same sample. (**B**) Retina sections containing $iP_{CAG}$-h-Rho transfected rods were co-labeled with anti-h-Rho mAb 3A6 and anti-(pan)-rhodopsin Ab C107, which recognizes both endogenous and transfected rhodopsins. We quantified the fluorescent intensities of 3 random areas in 23 transfected (Tf) rods and 23 non-transfected (non-Tf) rods immediately adjacent. The fluorescent intensity was expressed in arbitrary unit (a.u). Bars represent mean± standard deviation.

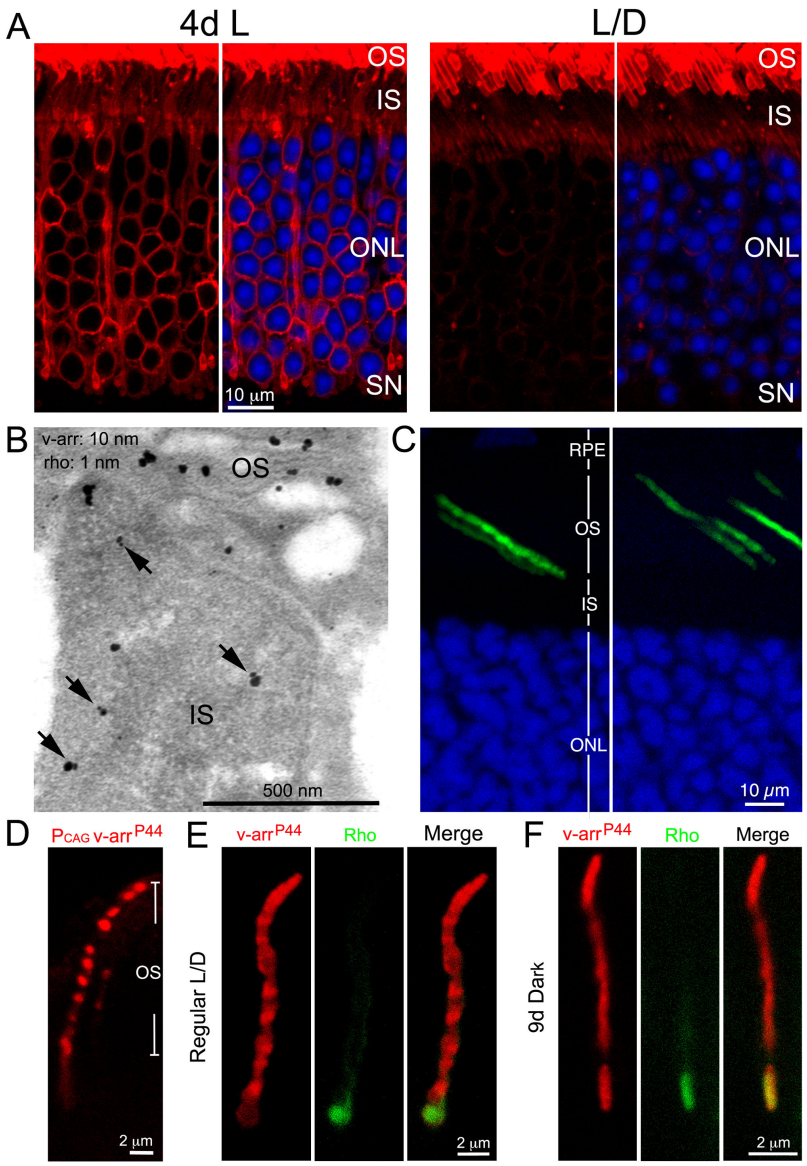


**Fig. S3 OS entry of endogenous rhodopsin follows a light-regulated pathway.** Related to Figure 3. (**A**) Immunolabeling of rhodopsin in retinas harvested from CD1 mice kept in 4-day constant room light (4dL) or normal light-dark cycles (L/D). Confocal images taken under identical conditions are shown. (**B**) A representative immunoEM image of endogenous rhodopsin (detected by 1-nm gold) and v-arr (detected by 10-nm gold) in light-adapted CD1 mouse rods. To visualize the gold particles, samples were silver-enhanced for 45 seconds. Arrows point to the colocalization of rhodopsin and v-arr. **(C)** $P_{CAG}$-GFP-v-arr transfected rods of rats kept in regular cyclic light until harvest; harvest was carried under the light. (**D**) Flag immuolabeling of $P_{CAG}$-Flag-v-arr$^{P44}$ transfected rods in rats kept in regular cyclic light until harvest. **(E-F)** Flag (red) and vsvg (green) immunolabeling of rods expressing i$P_{CAG}$-directed Flag-v-arr$^{P44}$ and vsvg-h-Rho for one day (via 4OH induction) and harvested under the light adapted conditions (~5000 lux, 30 min). Prior to the 4OH treatment, these rats that had been either continuously kept in regular light cycles (E) or in constant darkness for 9 days (F).

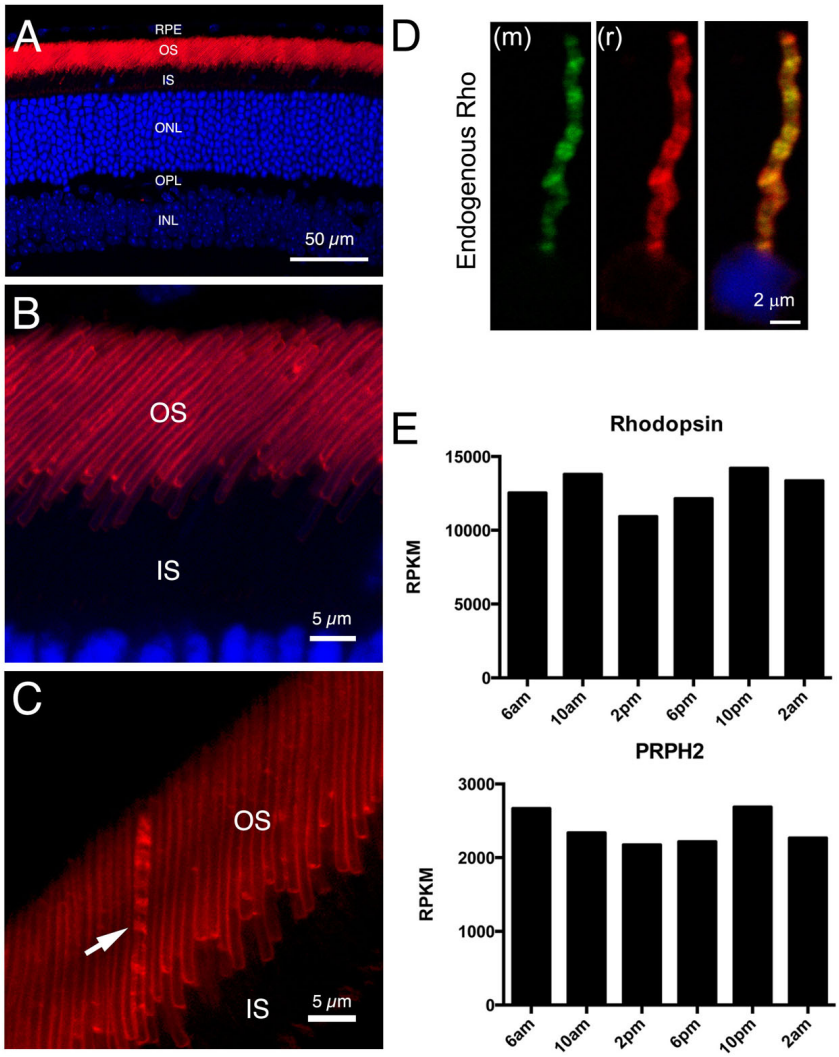


**Fig. S4 Expression analyses of endogenous OS proteins by immunostaining and RNAseq.** Related to Figure 4. Confocal images of low (A) and high (B, C) power views of a rat retinal slice stained with endogenous rhodopsin using B6-30 mAb. The optical depth is 0.5 μm (A and B) or 0.2 μm (C). As shown in B and C, nearly all rods exhibit robust rhodopsin immunolabeling on their plasma membranes (i.e., a "hollow" pattern) without significant labeling of the disc membranes inside the rod OS. An arrow points to a rod (in C) that displays a banding pattern inside the rod OS (arrow). We surmise that the surface of this particular rod OS was, by chance, better permeabilized, allowing the penetration of the Ab to access the rhodopsin expressed on the disc membranes inside the OS. (**D**) A representative confocal image of an individually dissociated rat rod that was double-labeled with a mouse (m) (i.e., K16-111C) and a rabbit (r) (i.e., C107 serum) anti-rhodopsin Ab. (**E**) Representative DeeqSeq data of three independent experiments is presented. In each repeat, two retinas of a C57BL/6J mouse were collected at indicated time points (6 am, 10 am, 2 pm, 6 pm, 10 pm, 2 am). Total RNA was subjected to RNA sequencing to evaluate gene expression quantified in units of RPKM (reads per kilobase of transcript per million mapped reads). The relative transcript levels of endogenous rhodopsin and PRPH2 expressed over the 6 time points of a day.

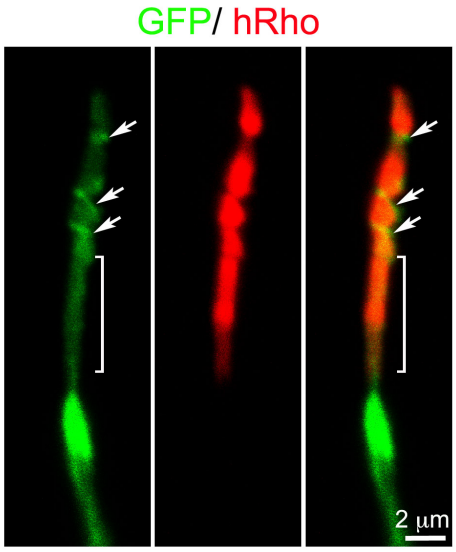


**Fig. S5. The periodicity of the OS cytostructure is altered by light.** Related to Figures 5 and 6. An example of representative rods transfected with $P_{CAG}$-directed hRho and GFP in rats reared in regular light cycle until 4-5 days prior to harvest, then moved to complete darkness. White arrows point to the GFP hotspots. Brackets indicate the proximal OS region in which strong h-Rho was homogeneously expressed and GFP hotspots were specifically lost.

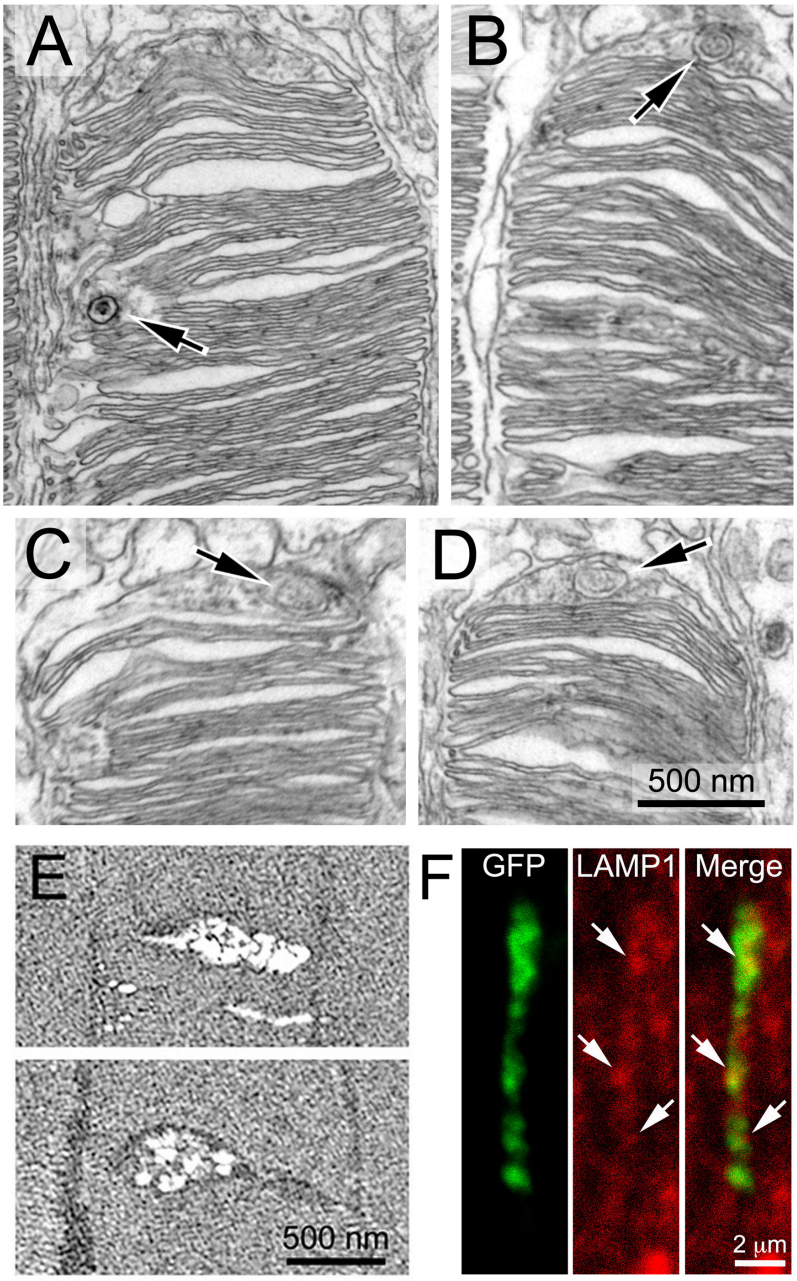


**Fig. S6. Distal OSCP contains MVB and autophagosome-like structure.** Related to Figure 7. **(A-D)** Electron micrographs show the distal OS regions of four representative rat rods. An enlarged view of Fig. 7B was shown in (A) to better reveal an MVB-like structure (i.e., a single-membrane structure containing intraluminal vesicles). (**B-D**) Arrows point to the morphologically characterized autophagosomes (i.e., double-membrane vacuoles enwrapping intraluminal vesicles and/or cytoplasmic materials). (**E**) Two representative block-face images from the FIM-SEM examination show views of OSCP (taken from 2 still images of Movie S4) in which vesicular and electron dense materials can be seen. (**F**) Colabeling of transfected GFP and LAMP1 showing that the two molecules have an overlapping distribution in the distal part of the OS (white arrows).

## SUPPLEMENTAL MOVIES

### Supplemental Movie Legends

**Movie S1. Spatial relationship between PRPH2 and h-Rho ectopically expressed in the rat rod. Related to Figure 4.** Animation of a maximum projection from confocal stacks of the same rod shown in Fig. 4C. This cell was co-transfected with $iP_{CAG}$-PRPH2-GFP and $iP_{CAG}$-h-Rho for 5 days. PRPH2-GFP was directly visualized by observing the green fluorescence (green); h-Rho was immunostained by anti-hRho 3A6 mAb (red).

**Movie S2. Spatial relationship between the h-Rho-rich discs and GFP-labeled cytoplasmic spaces. Related to Figure 5.** EndFragment
Animation of a maximum projection from confocal stacks of the same rod shown in Fig. 5B. The is a representative example of a rod OS that co-expressed $P_{CAG}$-GFP (green) and $P_{CAG}$-hRho (red).

**Movie S3. Spatial relationship between the GFP and h-Rho in transfected rod OS. Related to Figure 5.** EndFragment
Animation of a maximum projection from confocal stacks of a second example of a rod OS that co-expresses $P_{CAG}$-GFP (green) and $P_{CAG}$-hRho (red).

**Movie S4. Ultrastructural viewing of OSCP and disc heterogeneity in mouse rod OS. Related to Figure 6.** Animation of 22 consecutive block-face images of C57BL/6J mouse OS acquired by FIM-SEM. An arrow points to a characteristic OSCP. Brackets label several groups of discs that have porous appearance due to their enlarged cytoplasmic contacts.

## SUPPLEMENTAL EXPERIMENTAL PROCEDURES

### Abs

Anti-hRho mouse mAb 3A6 (Hodges et al., 1988), anti-rhodopsin C-terminus mAb1D4 (Molday and MacKenzie, 1983), anti-rat PRPH2-mouse mAbs 3B6, and anti-mouse PRPH2 mouse mAb 5H2 (Connell et al., 1991) were gifts from Robert Molday; anti-rhodopsin N-terminus mAb B6-30 and anti-rhodopsin C-terminus mAb K16-111C (Adamus et al., 1991). Rabbit anti-rhodopsin C-terminus Ab (C107) was generated in our lab (antigen: maltose binding protein fused with rhodopsin's C-terminal 39 residues; Cocalico Biochemicals, PA). Anti-Q344ter rabbit Ab was previously described (Sung et al., 1994); anti-prCAD rabbit Ab (Rattner et al., 2001). Additional primary Abs were anti-TGN38 mouse Ab (Affinity Bioreagents); anti-GFP chicken Ab (Abcam); anti-FLAG M2 mAb and polyclonal rabbit Ab (Sigma); anti-LAMP1 mouse mAb (clone AC17; gift from Enrique Rodriguez-Boulan (Nabi et al., 1991)); anti-vsvg mAb (clone P5D4; Abcam); anti-v-arr rabbit Ab (gift from Igal Gery; (Korf et al., 1985; Korf et al., 1986). Alexa-dye (Invitrogen) and immunogold (Electron Microscopy Sciences) conjugated secondary Abs were used.

### Plasmids

pCAG, pCAG-IRES-GFP, or pCAG-HcRed vectors were used for constitutive expression and pCALNL vector were used for inducible expression. These plasmids and plasmids encoding $ER^{T2}$-Cre-$ER^{T2}$ (under the CAG promoter) were gifts of Dr. Connie Cepko; (Matsuda and Cepko, 2004, 2007). PRPH2-mCherry and PRPH2-GFP had the fluorescent proteins tagged the C-terminus of bovine PRPH2 (Connell and Molday, 1990). GFP-v-arr (Chuang et al., 2004) as well as the Flag-v-$arr^{P44}$ (constructed by PCR amplifying the DNA fragment encoding the amino acids 1-370 of bovine v-arr) were inserted into CAG-loxP-neo-loxP. cDNAs containing human wild type rhodopsin (Chuang et al., 2004), Rho-GFP (Chuang et al., 2004), Rho-HcRed (this paper, see Fig.1B), R135L-GFP (Chuang et al., 2004), Flag-rhodopsin, vsvg-rhodopsin, PRPH2-GFP and Rab11a-GFP (gift of Dr. Tim MacGraw) were transferred into pCALNL downstream to the loxP-neo-STOP-loxP cassette. Plasmids encoding Cre driven by Nrl (i.e., $P_{Nrl}$) and rhodopsin (i.e., $P_{opsin}$) promoters (gifts of Connie Cepko; (Matsuda and Cepko, 2004) were used to generate the h-Rho expression construct.

### Immunohistochemistry of retinal sections

All transfected rats were harvested by transcardial perfusion with 4% PFA followed by postfixing with 4% PFA plus 0.1% glutaraldehyde overnight for most experiments. In some experiments (Figs 2B-2E, 3A-3C, 4A-4C) enucleated eyes were submerged in 4% PFA followed by 4% PFA/0.1% glutaldehyde post-fixation. Retinal pieces (3x2 mm) were embedded in 5% low-melting agarose, cut into 40 μm-thick vibratome sections, and then subjected to immunolabeling using standard free floating procedures (Chuang et al., 2007) with 0.25% Triton X-100 included in both blocking and primary Ab incubation. Washes were carried out in PBS containing calcium and magnesium. After the final washes, samples were mounted in Vectashield (Vector) or Prolong gold antifade reagent (Life technologies). For endogenous rhodopsin and PRPH2 staining, retinas were harvested under regular room light. In some experiments, sections were pretreated with neuraminidase (New England BioLabs) following the manufacturer's instructions prior to the primary Ab incubation. Briefly, sections were incubated in 0.25 unit/μL neuraminidase diluted in 0.1% TritonX-100 containing buffer for 30 mins at 37ºC. Sections were washed in PBS/0.1%TritonX-100 prior to standard blocking and Ab incubation procedures. All samples were analyzed by Leica TCS SP2 spectral confocal system. All confocal images shown in this paper have an optical depth between 0.2-0.5 μm.

**ImmunoEM of rodent rods**

CD1 mouse retinas were harvested by transcardial perfusion with 20 mL of 4% paraformaldehyde plus 0.1% glutaldehyde. Retina blocks were quenched in 0.1M glycine in PBS for 5 min, rinsed with PBS, followed by gradient dehydration in ethanol solutions. Retina blocks were then embedded in LR-White resin (Electron Microscopy Sciences) and kept at 50°C for 48 hours to polymerize. Ultrathin sections (70 nm) were cut and collected on nickel grids. After sections were collected, grids were heated at 60°C for 1 h to allow firmer attachment. Prior to immunolabeling procedures, grids were etched with 1% $H_2O_2$ for 10 min and rinsed 3-5 times in deionized water. For single Ab labeling, grids were blocked by 1% BSA/PBS and then incubated with primary Abs at room temperature overnight. Grids were washed in PBS and incubated with 10 nm gold-conjugated secondary Abs (Electron Microscopy Sciences) in PBS containing 1% BAS/fish gelatin (Amhersham Biosciences) at room temperature. After final washes in PBS and then water, grids were stained with uranyl acetate and lead citrate for final examination on a Philips CM10 electron microscope. For double immunolabeling, after the incubation of primary Ab mixture, 1 nm and 10 nm gold-conjugated secondary Abs were applied sequentially. Grids were then washed by PBS followed by 0.1M PB, 0.2M citrate buffer, and silver enhanced for 45 seconds using IntenSE M silver enhancement kit (GE Healthcare). Grids were immediately washed with fresh citrate buffer and water and air-dried, followed by uranyl acetate and lead citrate counter-staining and microscopy. In some experiments, electron micrographs (taken at 25,000x magnification) were collaged so that the longitudinal view of entire rod OS of several individual rods can be visualized. Each OS was divided into 116-180 fixed-width arbitrary units (a.u.) and the number of gold particles with each a.u. was counted.

## SUPPLEMENTAL REFERENCES


Adamus, G., Zam, Z.S., Arendt, A., Palczewski, K., McDowell, J.H., and Hargrave, P.A. (1991). Anti-rhodopsin monoclonal antibodies of defined specificity: characterization and application. Vision Res *31*, 17-31.

Chuang, J.Z., Vega, C., Jun, W., and Sung, C.H. (2004). Structural and functional impairment of endocytic pathways by retinitis pigmentosa mutant rhodopsin-arrestin complexes. J Clin Invest *114*, 131-140.

Chuang, J.Z., Zhao, Y., and Sung, C.H. (2007). SARA-regulated vesicular targeting underlies formation of the light-sensing organelle in mammalian rods. Cell *130*, 535-547.

Connell, G., B□ascom, R., Molday, L., Reid, D., McInnes, R., and Molday, R.S. (1991). Photoreceptor peripherin is the normal product of the gene responsible for retinal degeneration in the rds mouse. Proc Natl Acad Sci USA *88*, 723-726.

Connell, G.J., and Molday, R.S. (1990). Molecular cloning, primary structure, and orientation of the vertebrate photoreceptor cell protein peripherin in the rod outer segment disk membrane. Biochemistry *29*, 4691-4698.

Hodges, R.S., Heaton, R.J., Parker, J.M., Molday, L., and Molday, R. (1988). Antigen-antibody interaction: synthetic peptides define linear antigenic dterminants recognized by monoclonal antibodies directed to the cytoplasmic carboxy terminus of rhodopsin. J Biol Chem *263*, 11768-11775.

Korf, H.W., Moller, M., Gery, I., Zigler, J.S., and Klein, D.C. (1985). Immunocytochemical demonstration of retinal S-antigen in the pineal organ of four mammalian species. Cell and tissue research *239*, 81-85.

Korf, H.W., Oksche, A., Ekstrom, P., Gery, I., Zigler, J.S., Jr., and Klein, D.C. (1986). Pinealocyte projections into the mammalian brain revealed with S-antigen antiserum. Science *231*, 735-737.

Matsuda, T., and Cepko, C.L. (2004). INAUGURAL ARTICLE: Electroporation and RNA interference in the rodent retina in vivo and in vitro. Proc Natl Acad Sci U S A *101*, 16-22.

Matsuda, T., and Cepko, C.L. (2007). Controlled expression of transgenes introduced by in vivo electroporation. Proc Natl Acad Sci U S A *104*, 1027-1032.

Molday, R.S., and MacKenzie, D. (1983). Monoclonal antibody to rhodopsin: characterization, cross-reactivity and application as structural probes. Biochemistry *22*, 653-660.

Nabi, I.R., Bivic, A.L., Fambrough, D., and Rodriguez-Boulan, E. (1991). An endogenous MDCK lysosomal membrane glycoprotein is targeted basolaterally before delivery to lysosomes. J Cell Biology *115*, 1573-1584.

Rattner, A., Smallwood, P.M., Williams, J., Cooke, C., Savchenko, A., Lyubarsky, A., Pugh, E.N., and Nathans, J. (2001). A photoreceptor-specific cadherin is essential for the structural integrity of the outer segment and for photoreceptor survival. Neuron *32*, 775-786.

Sung, C.-H., Makino, C., Baylor, D., and Nathans, J. (1994). A rhodopsin gene mutation responsible for autosomal dominant retinitis pigmentosa results in a protein that is defective in localization to the photoreceptor outer segment. J Neuro *14*, 5818-5833.